Multi-modal breast imaging with ultrasound tomography

Neb Duric[1], Cuiping Li[1], Peter Littrup[1], Carri Glide-Hurst[1], Lianjie Huang[2], Jessica Lupinacci[1], Steven Schmidt[1] , Olsi Rama[1], Lisa Bey-Knight[1] and Yang Xu[1].
[1]Karmanos Cancer Institute, Wayne State University, 4100 John R. Street, Detroit, MI 48201
[2]Mail Stop D443, Los Alamos National Laboratory, Los Alamos, NM 87545

ABSTRACT

We report and discuss clinical breast imaging results obtained with operator independent ultrasound tomography. A series of breast exams are carried out using a recently upgraded clinical prototype designed and built on the principles of ultrasound tomography. The *in-vivo* performance of the prototype is assessed by imaging patients at the Karmanos Cancer Institute. Our techniques successfully demonstrate *in-vivo* tomographic imaging of breast architecture in both reflection and transmission imaging modes. These initial results indicate that operator-independent whole-breast imaging and the detection of cancerous breast masses are feasible using ultrasound tomography techniques. This approach has the potential to provide a low cost, non-invasive, and non-ionizing means of evaluating breast masses. Future work will concentrate on extending these results to larger trials.

Keywords: Breast imaging, breast masses, image fusion, ultrasound tomography

1. INTRODUCTION

Although mammography is the gold standard for breast imaging [1], its limitations result in a high rate of biopsies of benign lesions and a significant false negative rate for women with dense breasts [2]. Numerous ongoing studies are investigating alternative approaches including the large ACRIN study [3-5] aimed at evaluating the role of ultrasound in breast cancer screening. Ultrasound imaging has the advantage of being more comfortable than mammography (little or no compression) and also safer because it does not use ionizing radiation. Unlike mammography, however, conventional ultrasound has the drawback of being operator dependent. In an ongoing study at the Karmanos Cancer Institute, we are investigating the performance of an operator independent whole-breast ultrasound imaging system in a clinical setting. The purpose of this paper is to describe the study and to present and discuss *in vivo* breast imaging results.

2. METHODS

We have constructed and recently upgraded a clinical breast imaging prototype (Fig. 1) based on the principles of ultrasound tomography [6-13]. Patients lie face-down on a canvas bed such that the breast being imaged is suspended in a water bath (imaging tank) that is situated below the table surface. The breast is surrounded by a ring-shaped transducer that contains 256 equally spaced ultrasound elements. The elements are individually addressable and can be electronically switched between receive and transmit modes. Elements are sequentially fired to emit unfocused sound waves via a fan-shaped beam and signals are subsequently received on all 256 receivers. Each element has its own data acquisition channel so that the entire firing sequence can be achieved in about 0.3 seconds. The transducer is attached to a motorized gantry so that it can be translated in the vertical direction relative to the suspended breast. For a typical patient exam, the starting position of the transducer is at the patient's chest wall. The transducer is then translated downward, in incremental steps, to cover the entire breast. Data are collected at each step and correspond to a cross-sectional plane of the breast. The data acquisition procedure is illustrated in Figs. 1-2. Typically, 45 to 75 vertical transducer positions are used.

Medical Imaging 2008: Ultrasonic Imaging and Signal Processing, edited by Stephen A. McAleavey, Jan D'hooge, Proc. of SPIE Vol. 6920, 69200O, (2008) · 1605-7422/08/$18 · doi: 10.1117/12.772203

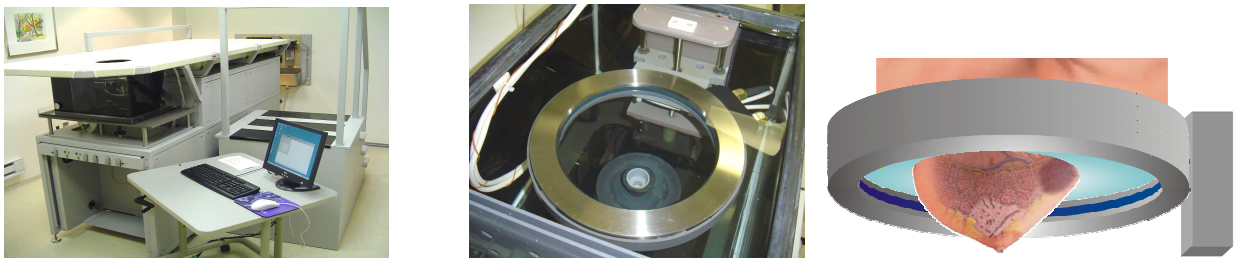

Figure 1. Experimental setup (left) and close-up of ultrasound ring transducer (center)**.** The ring transducer surrounds the breast. Both are immersed in water. The initial position of the transducer is at the chest wall. The transducer is then translated in incremental steps, to cover the entire breast (right). Data are collected at each step.

The *in-vivo* performance of the prototype is being assessed by imaging patients at the Karmanos Cancer Institute's Alexander J. Walt Comprehensive Breast Center. Patients are recruited on the basis of having suspicious masses on mammography and are subsequently examined with the prototype. All imaging procedures are performed under an Institutional Review Board (IRB) approved protocol and in compliance with the Health Insurance Portability and Accountability Act (HIPAA).

3. 3-D VOLUMETRIC IMAGING

The data acquired at each position of the transducer are used to construct cross-sectional images (tomograms) of the breast. A sample sequence of such ultrasound tomograms is shown in Fig. 2. Since the transducer position is encoded, the tomograms are automatically calibrated and, therefore, can be stacked together to represent a 3-D volume. The resulting image stacks can then be used to render volumetric images of the breast. An example of a volume rendering is shown in Fig. 3. The ability to render 3-D images is a direct result of the operator-independent nature of the breast scan.

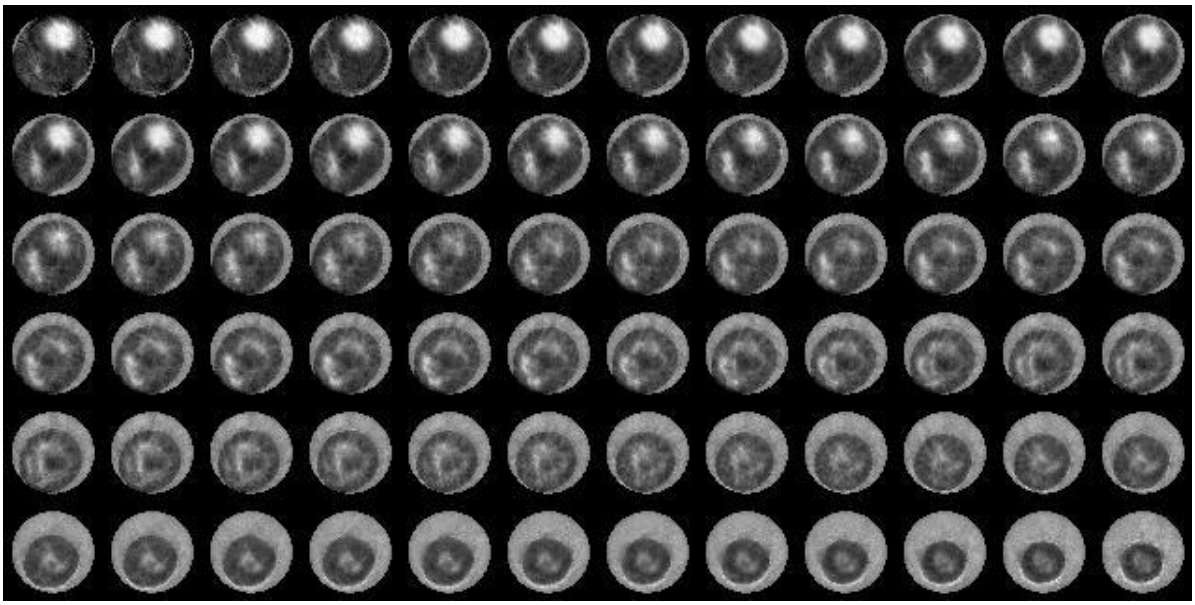

Figure 2. Reconstructions from data taken at 72 vertical positions of the transducer. From top left to bottom right, tomograms represent cross sections of the breast starting near the chest well and ending near the nipple. The outer white areas of the circular regions represent the water in which the breast is immersed. The darker regions represent breast tissue while the light regions inside the breast are masses and other dense breast tissues.

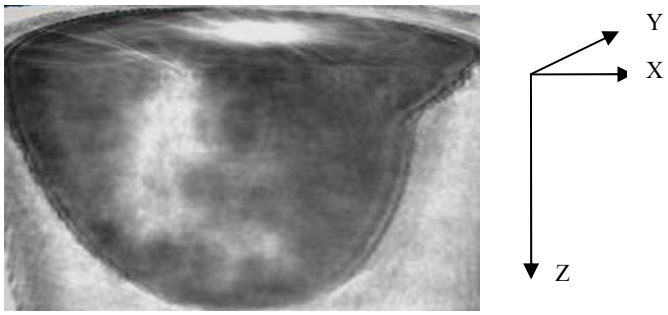

Figure 3. Volume rendering from a stack of ultrasound tomograms. This cut-away view shows a cross section of the breast near the chest wall (top of image) and a vertical cut through the remainder of the breast. The voxels that make up this 3-D image are 1mm x 1 mm x 1mm, in size. The spatial resolution is 2mm x 2mm x 4mm (X x Y x Z, as shown).

4. MULTI-MODAL IMAGING

A consequence of using a ring geometry that surrounds the breast is that it is possible to perform both reflection and transmission imaging. The reflection imaging is analogous to standard B-mode ultrasound imaging in that reflecting surfaces of internal breast tissue are imaged, as shown in Fig. 4a. The transmission imaging offers the possibility of imaging other tissue parameters such as sound speed and attenuation. An example of a transmission image is shown in Fig. 4b.

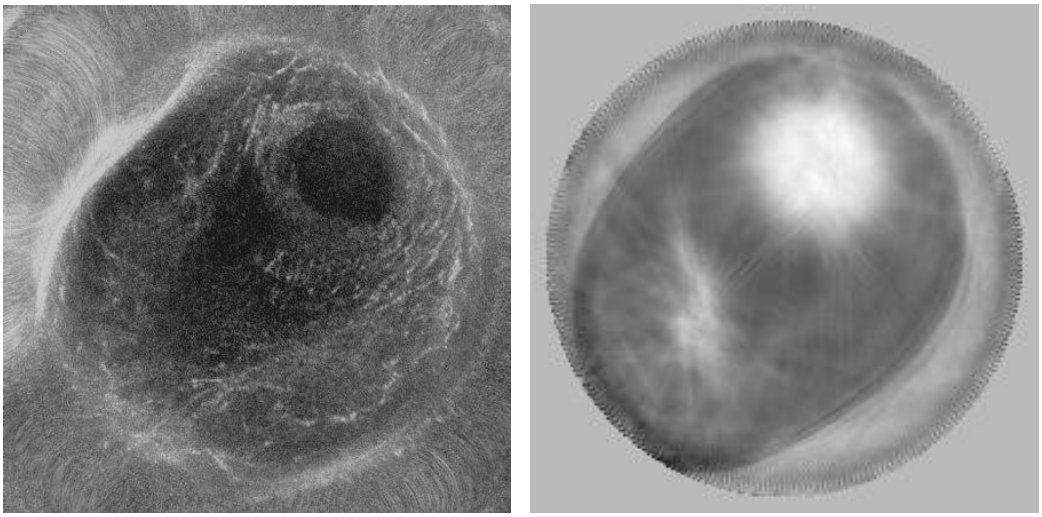

Figure 4. Examples of (a) reflection (left) and (b) transmission image (right) showing cross sectional images of the breast and a large cancer at the 1:00 o'clock position.

5. FUSION IMAGING AND CHARACTERIZATION

Reconstructions based on reflection and transmission imaging are used to generate images of reflection, sound speed and attenuation for every patient in the study, so that a volumetric assessment of each parameter could be undertaken. The motivation for this approach is to determine whether the measurement of multiple parameters can be used to characterize breast tissue [13] and thereby improve the specificity and sensitivity of the exam relative to standard US and mammography, each of which is based on single parameter imaging. An example of multi-parameter imaging is shown in Fig. 5.

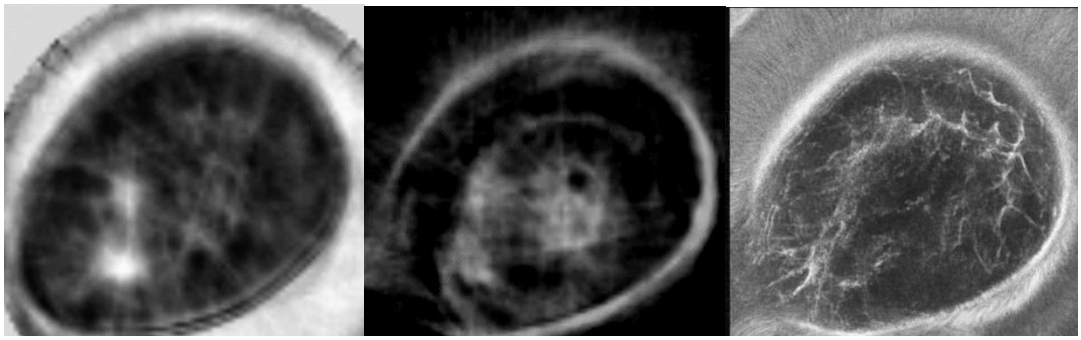

Figure 5. Examples of reflection and transmission images. Left: sound speed image. Center: attenuation image. Right: Reflection image.

Visual characterization of tissue can be implemented through the process of image fusion. We use the primary RGB colors to represent each of the three parameters of reflection, sound speed and attenuation, respectively, for the data shown in Fig. 6. A false color image, obtained by fusing the three images together, represents all three parameters. A visual representation of such characterization is shown in Fig. 6.

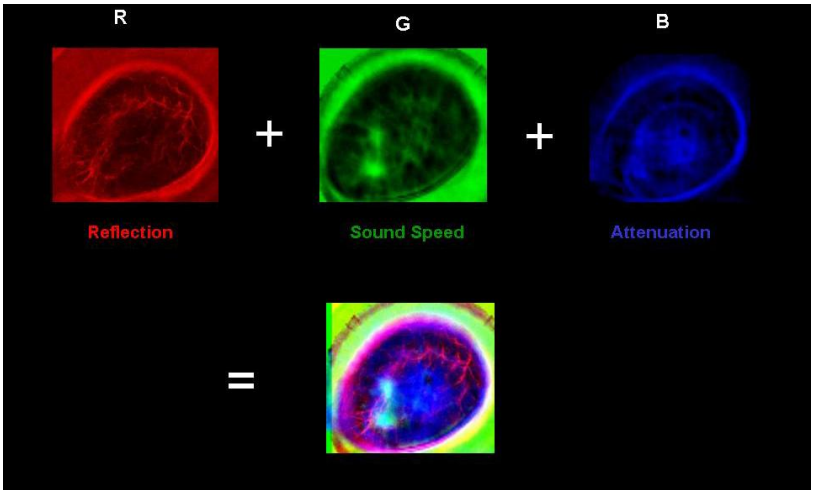

Figure 6. Top: Reflection (red), sound speed (green) and attenuation (blue) images. Bottom: Fusion images obtained by fusing the above images.

6. RESULTS

Examples of multi-parameter imaging and image fusion are shown in Figs. 7 and 8. An examination of the images shown in those figures reveals 4 components of breast tissue. The underlying *fatty tissue* presents itself as regions of low sound speed (dark) and low attenuation (dark). The denser *glandular tissue* has higher sound speed and appears lighter. Similarly, the higher attenuation levels indicate a lighter appearance in the attenuation images. Both types of images highlight the denser tissue. On the other hand, the reflection images trace the reflecting interfaces associated with *fibrous stroma* of the breast. All three images are sensitive to the presence of *masses* which show up as regions of high sound speed and/or high attenuation. Their appearance in the reflection images is usually manifested as a combination of local changes in echotexture and/or a distortion of the fibrous stroma, often referred to as architectural distortion. An examination of the fusion images in Figs. 7-8 shows that the components of the breast can be segregated by color such that the fatty regions present dark shades of red, glandular tissue is bluish and stromal structure is bright red. The masses tend to show up as cyan in color because of the contributions of sound speed and attenuation.

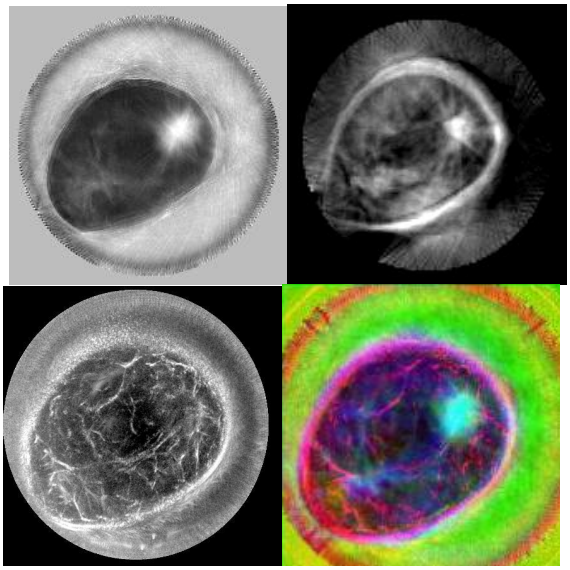

Figure 7. Cancer mass shows up as a high sound speed (top left), high attenuation (top right) region at the 2 o'clock far position. Reflection image (bottom) reveals some disruption of fibrous stroma. The fusion image (bottom right) combines these observations.

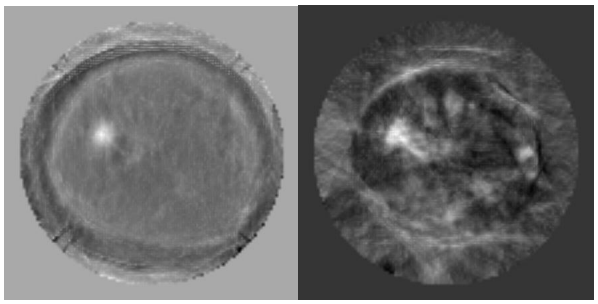

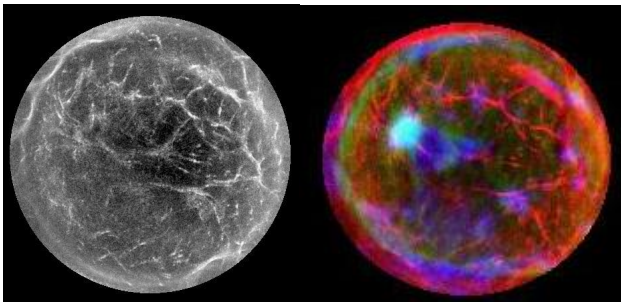

Figure 8. Cancer mass shows up as a high sound speed (top left), high attenuation (top right) region at the 10 o'clock mid position. The fusion image (bottom right) combines these observations.

7. DETECTION AND CHARACTERIZATION OF BREAST MASSES

To date, over 200 patients have been imaged with the ultrasound tomography prototype. The ability to image multiple tissue parameters has led us to investigate the use of reflection, sound speed and attenuation parameters to characterize breast masses in this sample of patients. The methodology we are pursuing can be visualized with the following illustrative examples.

Multi-parameter images of a cyst. Figure 9 shows reconstructions of reflection, sound speed and attenuation images for a cross-section of a breast containing a cyst.

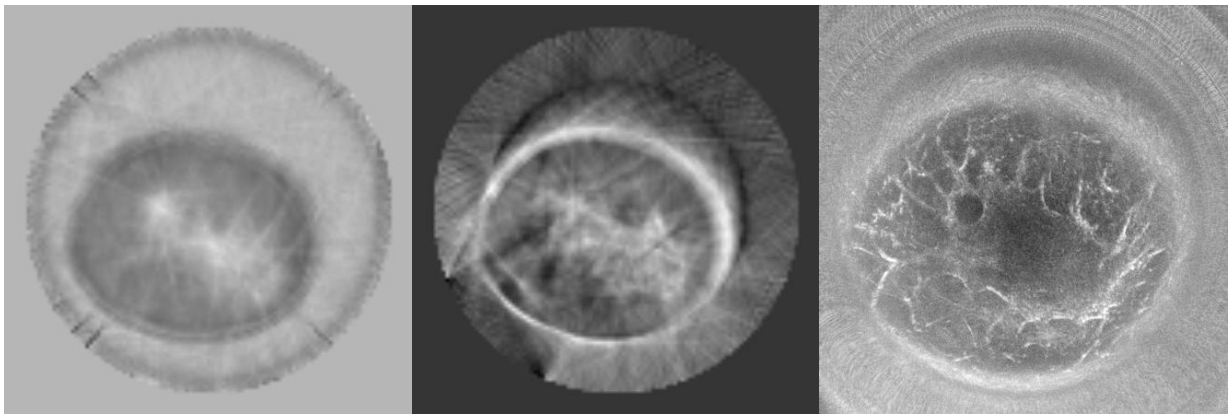

Figure 9. From left to right, sound speed, attenuation and reflection images of a 10 mm sized cyst in approximately the 10 o'clock, mid position of the breast..

The cyst appears as a round, anechoic region on the reflection images, similar to its appearance on standard ultrasound images. The sound speed image shows a slight local elevation in sound speed. However, no distinct elevated attenuation region is evident relative to background tissue. The latter is to be expected because cysts should have minimal attenuation owing to their largely liquid nature. The elevated sound speed is the result of the fact that water at body temperature (sound speed of ~ 1.5 mm/μs) has a higher sound speed than fat.

Multi-parameter images of a Fibroadenoma. Figure 10 illustrates the properties of a fibroadenoma. Shown are reflection, sound speed and attenuation images of a 1cm fibroadenoma at approximately the 2 o'clock position.

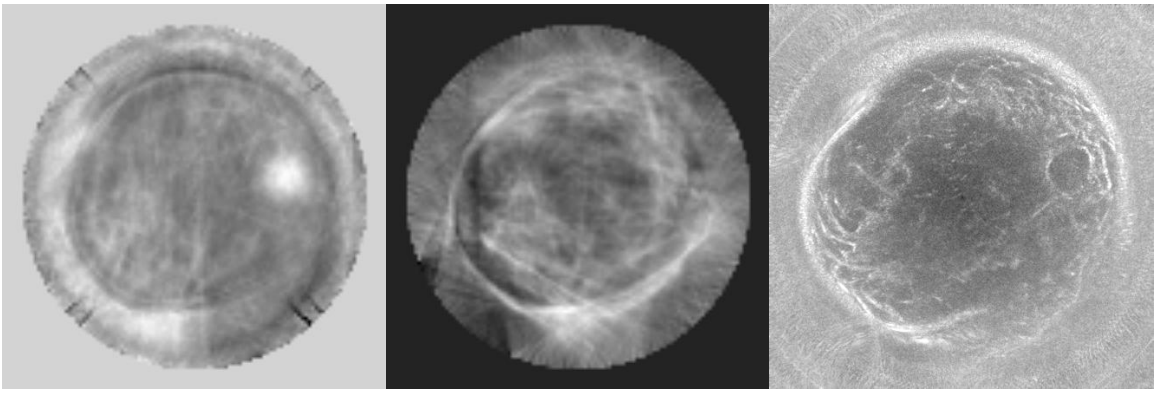

Figure 10: From left to right, sound speed, attenuation and reflection images of a fibroadenoma in approximately the 2 o'clock, far position of the breast.

The fibradenoma appears as an oval, slightly hypoechoic region on the reflection images, similar to its appearance on standard ultrasound images. The sound speed image shows a strong local elevation in sound speed. However, no distinct elevated attenuation region is evident relative to background tissue. .

Multi-parameter images of a cancer. Figure 11 shows analogous images for a cancer. The 2.5 cm mass, located in approximately the 12 o'clock near position, demonstrates hypoechoic texture in reflection, and elevated sound speed and attenuation. Unlike the benign cysts noted above, the characteristics of the cancer deviate from those of the benign masses. The most obvious difference is the elevated attenuation relative to background tissue.

Current work is aimed at quantifying these differences using our data collected from 200 patients. We are in the process of collecting multiple mass properties from these three types of images with the goal of constructing a predictive model that will then be applied in a prospective study to determine how well benign masses can be differentiated from cancer.

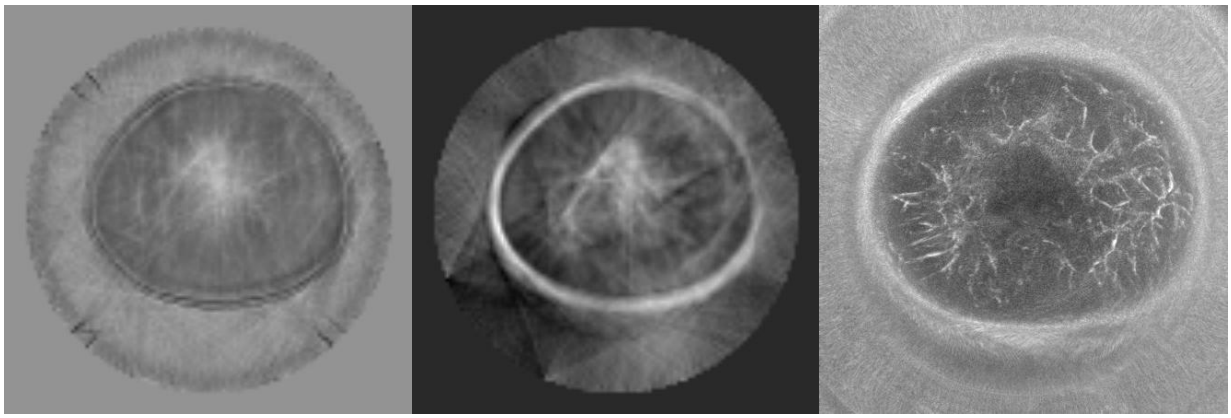

Figure 11. From left to right, sounds speed, attenuation and reflection images of a 2.5 cm sized cancer in approximately the 12 o'clock, near position of the breast.

8. CONCLUSIONS

Analyses of clinical breast images reconstructed from simultaneous acquisitions of reflection and transmission data are presented. These results indicate that operator-independent whole-breast imaging and the detection of cancerous breast masses are feasible using ultrasound tomography techniques. Our techniques successfully demonstrate tomographic imaging of breast architecture using reflection and transmission imaging modes. The ability to image the entire volume of the breast is also demonstrated. Reflection, sound speed, and attenuation imaging of breast masses are demonstrated *in vivo*. Future studies will focus on quantifying the sensitivity and specificity of our approach relative to conventional ultrasound and mammography.

9. REFERENCES

[1] Berry DA, et al., "Effect of Screening and Adjuvant Therapy on Mortality from Breast Cancer", N Engl J Med. , 1784 (2005).

[2] Gotzsche PC, Olsen O. "Is screening for breast cancer with mammography justifiable?" Lancet 355, 129-134 (2000).

[3] Kolb, T.M., Lichy, J. and Newhouse, J.H. "Comparison of the Performance of Screening Mammography, Physical Examination, and Breast US and Evaluation of Factors that Influence Them: An Analysis of 27,825 Patient Evaluation", Radiology 225, 165 - 175 (2002).

[4] Lucas-Fehm, L. "Sonographic mammographic correlation", Applied Radiology, 20-25 (2005).

[5] ACRIN, "website: www.acrin.org", (2008).

[6] Norton SJ, Linzer M. "Ultrasonic reflectivity tomography: reconstruction with circular transducer arrays", Ultrason Imaging 2, 154-84 (1978).

[7] Carson PL, Meyer CR, Scherzinger AL, Oughton TV "Breast imaging in coronal planes with simultaneous pulse echo and transmission ultrasound", Science 214, 1141-3 (1981).

[8] M. P. Andre, H.S. Janee, P. J. Martin, G. P. Otto, B. A. Spivey, D. A. Palmer, "High-speed data acquisition in a diffraction tomography system employing large-scale toroidal arrays," International Journal of Imaging Systems and Technology 8 137-147 (1997).

[9] Johnson S. A., Borup, D. T., Wiskin J. W., Natterer F., Wuebbling F., Zhang Y., Olsen C. "Apparatus and Method for Imaging with Wavefields using Inverse Scattering Techniques" United States Patent 6005916, (1999).

[10] Marmarelis, V.Z., Kim, T., Shehada, R.E. "Ultrasonic Imaging and Signal Processing", Proceedings of the SPIE: Medical Imaging, Paper 5035-6(2002).

[11] Liu, D.-L., and Waag, R. C. "Propagation and backpropagation for ultrasonic wavefront design", IEEE Trans. on Ultras. Ferro. and Freq. Contr. 44(1), 1-13 (1997).

[12] Duric, N., Littrup, P., Poulo, L., Babkin, A., Pevzner, R., Holsapple, E., Rama, O., Glide, C. "Detection of Breast Cancer With Ultrasound Tomography: First Results with the Computerized Ultrasound Risk Evaluation (C.U.R.E) Prototype", Medical Physics 34 (2), 773-785 (2007).

[13] J. F. Greenleaf, A. Johnson, R. C. Bahn, B. Rajagopalan "Quantitative cross-sectional imaging of ultrasound parameters", Ultrasonics Symposium Proc., IEEE Cat. # 77CH1264-1SU, 989-995 (1977).